SCALING LAWS FOR THE PERFORMANCE OF RIGID PROPULSORS INTENDED FOR UNDERWATER LOCOMOTION

Daniel Floryan

Mechanical and Aerospace Engineering
Princeton University
Princeton, NJ 08544, USA
dfloryan@princeton.edu

Tyler Van Buren

Mechanical and Aerospace Engineering
Princeton University
Princeton, NJ 08544, USA
tburen@princeton.edu

Clarence W. Rowley

Mechanical and Aerospace Engineering
Princeton University
Princeton, NJ 08544, USA
cwrowley@princeton.edu

Alexander J. Smits

Mechanical and Aerospace Engineering
Princeton University
Princeton, NJ 08544, USA
asmits@princeton.edu

ABSTRACT

Scaling laws are presented for the propulsive performance of rigid foils undergoing oscillatory motion in water. Water tunnel experiments on a nominally two-dimensional foil show that the scaling laws provide an excellent description of the data for thrust, power, and efficiency. The scaling laws are then extended to account for the effects of non-sinusoidal motions by using a parameter based on the maximum velocity of the trailing edge, which describes the experiments on non-sinusoidal gaits described by Jacobi elliptic functions reasonably well. Lastly, intermittent motions are considered. The thrust and power is shown to scale linearly with the duty cycle, and scaling laws for the energetics are presented. Intermittent motions are generally energetically advantageous over continuous motions, unless metabolic energy losses are sufficiently high.

INTRODUCTION

The flow around moving foils serves as an abstraction of many interesting swimming and flight problems observed in nature. Our interests lie mainly in exploiting the motion of foils for the purpose of propulsion, and so we shall focus on the thrust they produce, as well as how efficiently they perform. We confine our attention to rigid, nominally two-dimensional foils in pitching or heaving motions. We consider three types of gait: sinusoidal continuous, non-sinusoidal continuous, and sinusoidal intermittent.

Analytical treatments of pitching and heaving (sometimes called plunging) foils date back to the early-mid 20th century. Garrick (1936) extended the linear, inviscid, and unsteady theory of Theodorsen (1935) to provide expressions for the mean thrust produced by an oscillating foil, as well as the mean power input and output. Lighthill (1970) extended the theory to undulatory motion in what is called elongated-body theory. Although these treatments are analytic, it is difficult to extract physical insights from them in regards to mean fluid quantities like thrust.

Scaling laws, although lacking the precision and technicality of the aforementioned approaches, often provide meaningful physics responsible for observed fluid phenomena, and have been used for this problem as well. Triantafyllou *et al.* (2005) reviews the available scaling laws in aquatic locomotion and fishlike swimming. The Strouhal number has been adapted as the main parameter of interest in nearly all works on swimming flows. Studies on propulsors with significant flexibility have adopted the reduced frequency as a very important parameter (Dewey *et al.*, 2013). We find, however, that these flows cannot be described by one parameter alone. We therefore find it necessary to revisit the problem, in particular how the propulsive performance scales with the available parameters. We seek scaling laws that are simple, explain the observed propulsive performance, and are directly connected to the underlying physical phenomena.

Here, we examine three types of motion: the first comprises canonical sinusoidal heaving and pitching motions; the second comprises a one-parameter family of non-sinusoidal heaving and pitching motions; and the third comprises intermittent motions (alternating periods of swimming and rest).

SINUSOIDAL, CONTINUOUS MOTIONS

We consider a rigid two-dimensional foil undergoing heave and pitch oscillations about its leading edge. The motions are described by $h(t) = h_0 \sin(2\pi f t)$ and $\theta(t) = \theta_0 \sin(2\pi f t)$, respectively, where h_0 is the heave amplitude, θ_0 is the pitch amplitude, and f is the frequency of oscillation. The foil moves horizontally at a constant speed U_∞, and the motion of the foil causes the surrounding fluid to impart forces onto it. We are chiefly concerned with the time-averaged thrust coefficient, C_T, produced by the foil, the power input coefficient, C_P, and the efficiency of the thrust production, $\eta = C_T/C_P$. Here,

$$C_T = \frac{F_x}{\frac{1}{2}\rho U_\infty^2 sc}, \qquad C_P = \frac{F_y\dot{h} + M\dot{\theta}}{\frac{1}{2}\rho U_\infty^3 sc},$$

where F_x is the force produced in the streamwise direction (thrust), F_y is the force produced in the transverse direction, M is the moment about the leading edge, and s is the span of the foil. The relevant dimensionless parameters are the reduced frequency, $f^* = fc/U_\infty$, and the Strouhal number, $St = 2fA/U_\infty$, where c is the chord, and A is the amplitude of the trailing edge motion of the foil.

By only considering quasi-steady lift and added mass forces, Floryan *et al.* (2017*a*) arrived at scaling laws for the thrust, power,

and efficiency. For heaving motions they found

$$\begin{aligned} C_T &= c_1 St^2 + c_2 St^2 f^* U^* - C_{Dh}, \\ C_P &= c_3 St^2 + c_4 St^2 f^* + c_5 St^2 f^* U^*, \\ \eta &= \frac{c_1 + c_2 f^* U^*}{c_3 + c_4 f^* + c_5 f^* U^*}, \end{aligned} \tag{1}$$

where $U^* = U_\infty / U_{\text{eff}} = 1/\sqrt{1+\pi^2 St^2}$ is the ratio of the freestream velocity to that seen by the foil. For pitching motions they similarly obtained

$$\begin{aligned} C_T &= c_6 St^2 + c_7 St A^* - C_{Dp}, \\ C_P &= c_8 St^2 + c_9 St^2 f^*, \\ \eta &= \frac{1}{f^*} \frac{c_6 f^* + c_7/2}{c_9 f^* + c_8}. \end{aligned} \tag{2}$$

C_{Dh} and C_{Dp} are the drag coefficients for heave and thrust, respectively, and the expressions for efficiency only hold in the limit of negligible drag. The constants c_1 to c_9 need to be found empirically.

These scaling laws were verified by Floryan *et al.* (2017*a*) through experiments on a heaving and pitching foil in a water tunnel, shown schematically in figure 1. A teardrop foil was used, with a chord of $c = 80$ mm, maximum thickness $t = 8$ mm, and span of $s = 279$ mm. The foil extended the entire depth of the water channel, and was considered to be effectively two-dimensional. The tunnel velocity was fixed at $U_\infty = 60$ mm/s, yielding a chord-based Reynolds number of $Re = 4780$. Planar baffles were installed upstream and downstream of the foil to eliminate free surface effects. Forces and torques were measured directly via a six-component force and torque sensor.

The empirical constants were determined to be $c_1 = 3.52$, $c_2 = 3.69$, $C_{Dh} = 0.15$, $c_3 = 27.47$, $c_4 = 13.81$, $c_5 = 5.06$, $c_6 = 2.55$, $c_7 = 0$, $C_{Dp} = 0.08$, $c_8 = 7.78$, and $c_9 = 4.89$; we refer to Floryan *et al.* (2017*a*) for an interpretation of the values. Figure 2 shows the mean thrust and power for heave and pitch as functions of the scaling parameters. All of the data shows excellent collapse, indicating that the simplified physics of the model capture the essential features of the foil performance. That is, the mean output generated by the unsteady motions of the foil are captured well by the effects of added mass and the rate of change of angle of attack.

Figure 3 shows the efficiency for heaving and pitching motions. The dashed lines mark the inviscid scalings, and the solid lines mark the viscous scalings. We see that the heaving efficiency data approaches a constant value for higher values of reduced frequency. This trend is as expected since the viscous drag remains almost constant for these motions, and so viscous drag becomes less important as more intense motions produce more thrust. The story is the same for pitching motions. The pitching efficiency data follows the inviscid f^{*-1} scaling law, but deviates for less intense motions due to the viscous drag. We thus see the importance of including viscous drag in any modeling efforts, as it is the cause of the universally-seen sharp decrease in efficiency for less intense motions.

NON-SINUSOIDAL, CONTINUOUS MOTIONS

Here, we consider non-sinusoidal motions to determine if there might be performance benefits to be gained by shaping the actuation waveform. The literature on studies of waveform shape is not extensive, with the studies of Read *et al.* (2003) and Van Buren *et al.* (2017*a*) being some of the few relevant works. Van Buren *et al.* (2017*a*) considered motions described by Jacobi elliptic functions. Jacobi elliptic functions are convenient because they describe a wide range of waveforms with a single parameter, the elliptic modulus κ. The waveforms vary smoothly from approximately triangular ($\kappa = -1$), to perfectly sinusoidal ($\kappa = 0$), to approximately square ($\kappa = 1$). See Figure 4.

As shown by Van Buren *et al.* (2017*a*), square-like motions produce significantly more thrust and require significantly more power than sinusoidal motions, whereas triangle-like motions are more similar to sinusoidal motions. The thrust and power for different waveforms were found to correlate strongly with the maximum velocity of the trailing edge motion. Van Buren *et al.* (2017*a*) thus introduced a peak velocity parameter,

$$P_2 = b_1 \dot{a}^* + b_2 \dot{a}^{*2}, \tag{3}$$

to scale the thrust and power coefficients for different waveforms. Here, b_1 and b_2 are empirical constants and $\dot{a}^* = \dot{a}/\dot{a}_{\kappa=0}$ is the ratio of the peak velocity of a waveform to the peak velocity of a sinusoidal waveform, which only varies with elliptic modulus.

Figure 5 shows the results of combining the above peak velocity scale with the scaling laws (1) and (2). The frequencies and amplitudes studied are the same as for sinusoidal motions, but we have added triangle-like and square-like waveforms shown in Figure 4. We have kept the same values for the constants c_1-c_9 as before, and obtain an encouraging collapse of the thrust and power coefficients for a large range of motion parameters. It appears that the peak velocity of the trailing edge is the correct parameter to define the performance.

SINUSOIDAL, INTERMITTENT MOTIONS

We now consider intermittent motions. These motions are characterized by alternating periods of active swimming and rest. The proportion of time spent actively swimming is given by the duty cycle Δ. We consider sinusoidal pitching motions with amplitudes of $\theta_0 = 5^\circ$ to 15° every 5°, frequencies of $f = 0.2$ to 1.5 Hz every 0.1 Hz, and duty cycles of $\Delta = 0.2$ to 1.0 every 0.1, with $\Delta = 1$ corresponding to continuous motions. The freestream velocity was increased to $U_\infty = 100$ mm/s for these experiments to improve the accuracy of our force and torque measurements.

When fish swim intermittently (also called burst and coast motion), they flap their caudal fin to propel themselves forward, then stop flapping and coast for some time, slowing down as they do so, before starting flapping again. It might be expected that this strategy is energetically favorable Weihs (1974), but it is clear that the metabolic rate needs to be taken into account, where the metabolic rate represents the rate at which energy is required to perform all functions apart from swimming.

We begin by conducting experiments in which the foil is fixed in the streamwise direction. Although a swimmer would slow down during the rest portion of an intermittent motion, and we might expect that the change in velocity would alter the thrust and power measurements, it has been shown that such effects are small (Van Buren *et al.*, 2017*b*). We thus consider the results of our fixed-velocity experiments to be faithful representations of free-swimming results.

The time-averaged thrust and power coefficients are shown in figure 6, where we have scaled thrust and power by the duty cycle Δ. As shown by Floryan *et al.* (2017*b*), scaling by the duty cycle collapses the data for all of the duty cycles onto a single curve. This has the effect of correcting the time-averaging so that the averaging is only done on the active portion of the cycle. This result implies that the thrust and power generated in each actuation cycle can be treated independently.

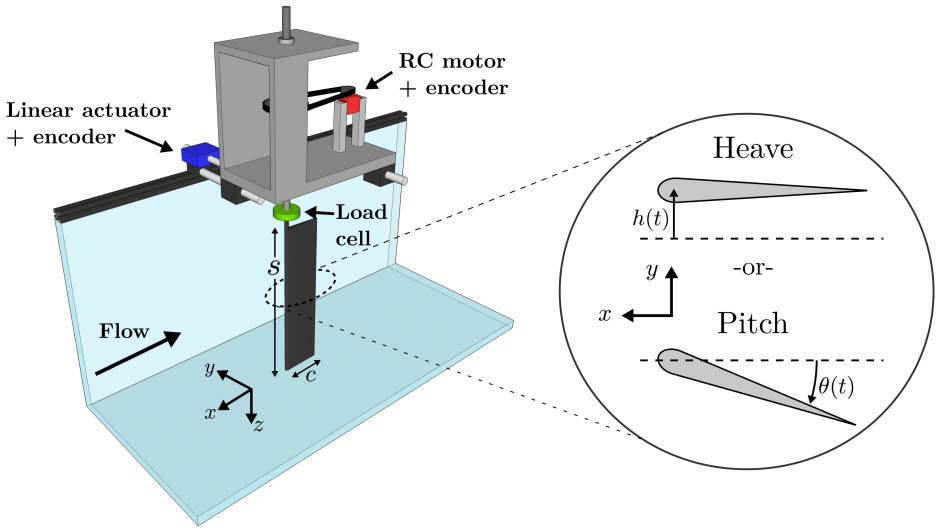

Figure 1. Experimental setup and sketch of motions.

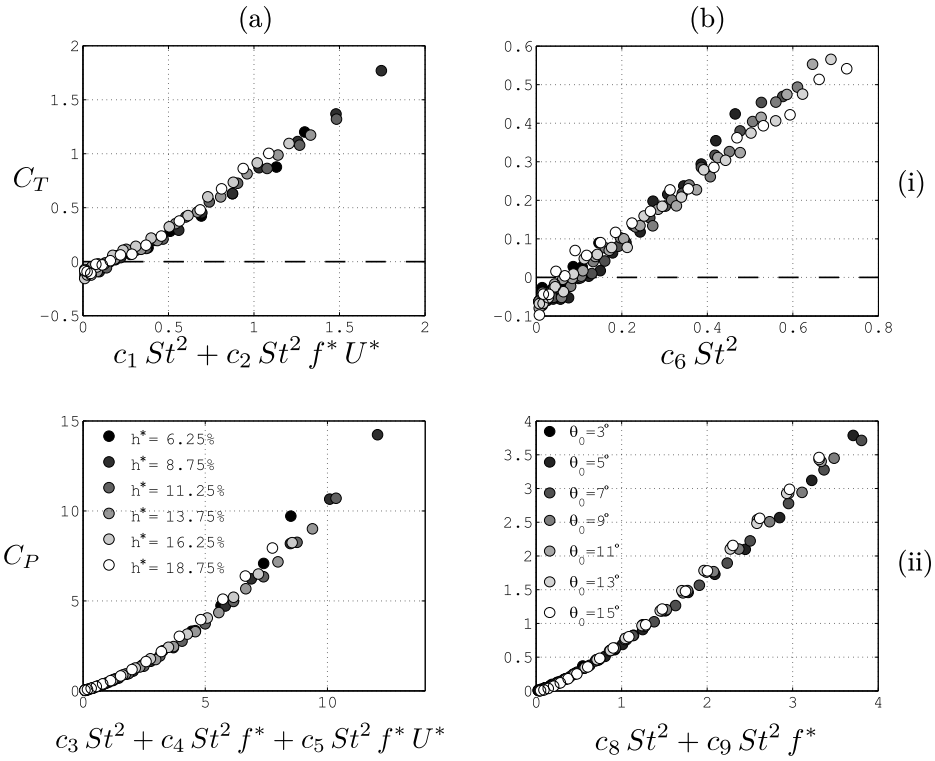

Figure 2. Time-averaged (i) thrust and (ii) power coefficients for (a) heave and (b) pitch as functions of the scaling parameters.

We also consider the energetic implications of intermittent motions. As originally shown by Weihs (1974) using a theoretical model, intermittent swimming motions may be energetically favorable compared to continuous motions. To study the energetics, we must consider a free swimmer (one whose velocity is allowed to change in accordance with the instantaneous forces felt). We solve for the free swimming velocity by integrating

$$m\dot{u} = T - D \tag{4}$$

numerically. Here, m is the mass of the swimmer, u is its time-varying velocity, T is the thrust that we have measured experimentally, and $D = \rho u^2 A_w C_D/2$ is the drag, with A_w being the wetted area of the swimmer and C_D its drag coefficient. The problem is described in more detail in Floryan *et al.* (2017*b*). By way of example, we set the mass and area ratios equal to $m^* = m/\rho c^2 s = 1$ and $A_w^* = A_w/sc = 10$, respectively, where s is the span of the propulsor, and we set the drag coefficient to $C_D = 0.01$ (Barrett *et al.*, 1999).

Given a set of actuation parameters (frequency and amplitude), we would like to know whether changing the duty cycle decreases the energy required to travel a certain distance. We consider both the energy required for swimming, as well as metabolic energy losses. The energetic benefits of intermittent swimming are captured by the

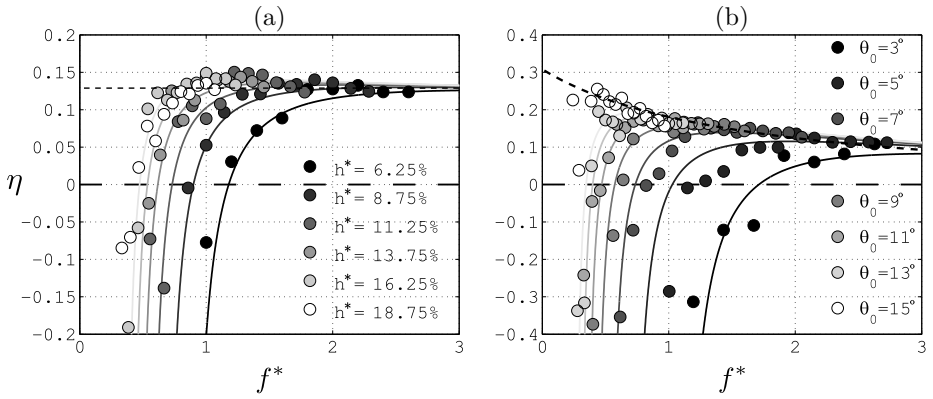

Figure 3. Efficiency for (a) heave and (b) pitch. Solid lines indicate the viscous scaling, and dashed lines indicate the inviscid scaling (taking the drag coefficient to be zero).

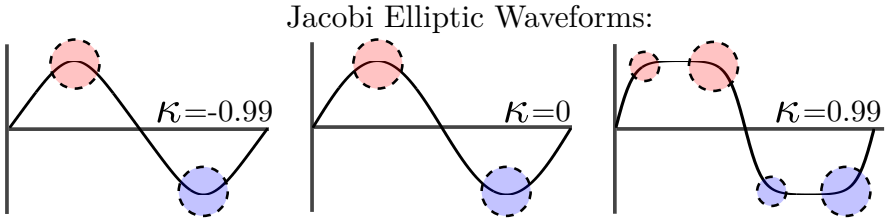

Figure 4. Jacobi elliptic functions produce varying actuation waveform shape based on the elliptic modulus, κ. Colored circles represent points of vortex production in the cycle based on PIV measurements, and smaller circles correspond to secondary vortices (see Van Buren *et al.* (2017*a*)).

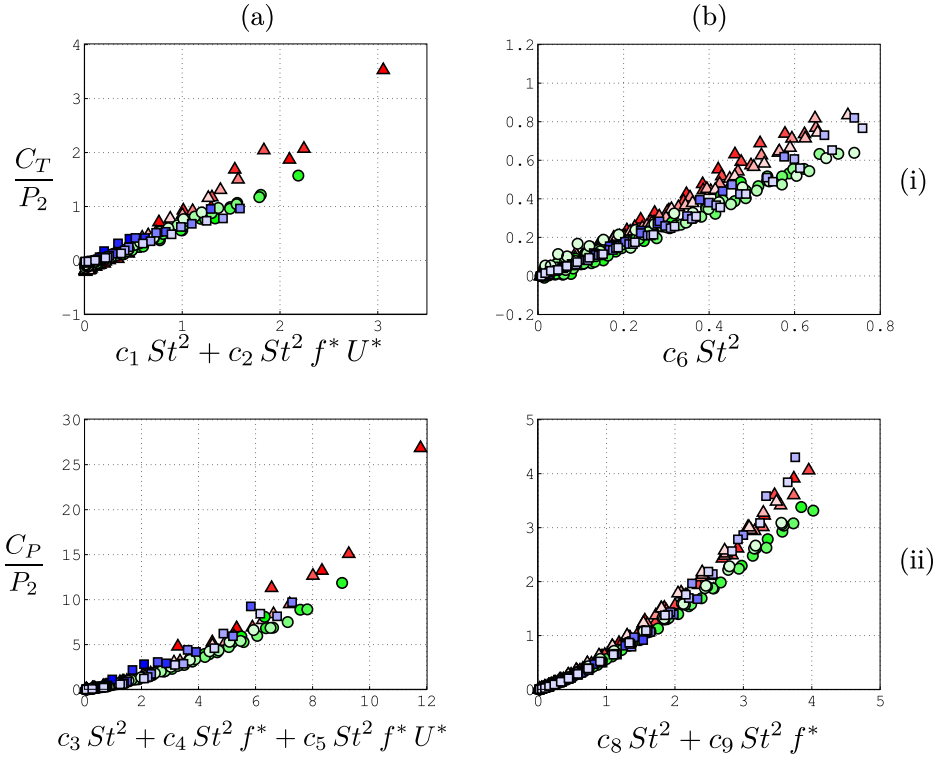

Figure 5. Time-averaged (i) thrust and (ii) power coefficients modified by the lateral velocity scale for (a) heave and (b) pitch as functions of the scaling parameters. Symbol color identifies the waveform shape: red is triangle-like, green is sinusoidal, and blue is square-like. Tone represents amplitude, ranging from low (dark) to high (light). Coefficient values are: (a.i) $b_1 = 0.4$, $b_2 = 0.8$; (a.ii) $b_1 = 0.4$, $b_2 = 0.8$; (b.i) $b_1 = 1$, $b_2 = 0$; and (b.ii) $b_1 = 0.8$, $b_2 = 0.3$.

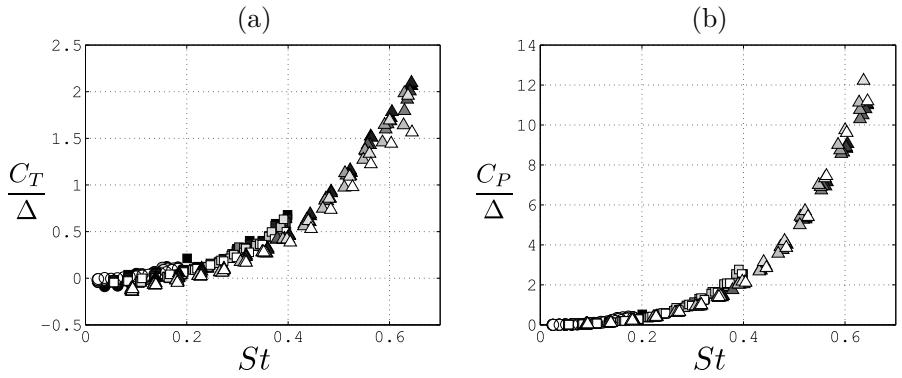

Figure 6. Time-averaged (a) thrust and (b) power coefficients normalized by duty cycle as functions of Strouhal number. Dark to light symbols represent increasing duty cycles, ranging from $\Delta = 0.2$ to 1 every 0.1. Symbols identify pitch amplitudes of $\theta_0 = 5^\circ$ (circle), 10° (square), and 15° (triangle).

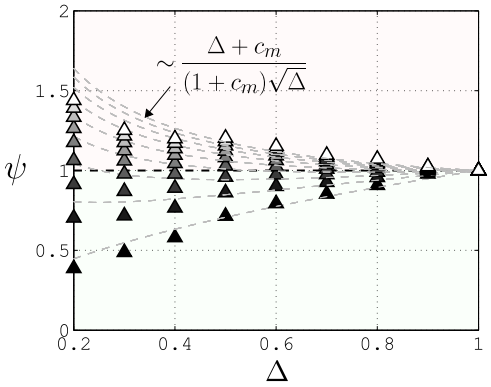

Figure 7. Ratio of energy expended by intermittent motions to energy expended by continuous motions, including metabolic energy losses, as a function of duty cycle for $\theta_0 = 15^\circ$, all frequencies, $m^* = 1$, and $A_w^* = 10$. Each point is an average over all frequencies. The color denotes the value of the metabolic power fraction c_m, 0 to 2 in intervals of 0.25 (dark to light).

energy ratio

$$\psi = \frac{E + E_m}{E_0 + E_{m0}}, \tag{5}$$

where E describes swimming energy losses, E_m describes metabolic energy losses, and subscript 0 denotes continuous swimming. Values of $\psi < 1$ indicate motions that are energetically favorable. We assume that the mean power spent on metabolic processes is the same for continuous and intermittent motions, and that it is a constant fraction c_m of the power lost in continuous swimming, that is, $P_m = c_m P_0$. The experimental results are plotted in figure 7. We have varied the metabolic power fraction c_m from 0 to 2, values that are typical in biology (Di Santo and Lauder, private communication). With $c_m = 0$ (darkest symbols), intermittent motions are always energetically favorable. This makes sense since a swimmer in this scenario does not expend any energy during the inactive portion of intermittent motions, but still coasts forward, so that the intermittent motions are always energetically favorable. As the metabolic power fraction is increases, however, the trend is reversed. For large enough c_m, intermittent motions expend more energy than continuous motions.

Based on the linear scaling of the mean thrust and power with the duty cycle, Floryan *et al.* (2017*b*) showed that the energy ratio should scale as

$$\psi = \frac{\Delta + c_m}{(1+c_m)\sqrt{\Delta}}. \tag{6}$$

From figure 7, the data and scaling tell the same story. As metabolic energy losses increase, intermittent motions can become energetically disadvantageous. Even though intermittent motions expend less energy on swimming, the metabolic losses can play a significant role because intermittent motions take more time to traverse a given distance than continuous motions. The extra time to travel will increase the metabolic energy losses, and this effect may become dominant.

CONCLUSIONS

Using an analysis based only on quasi-steady lift-based and added mass forces, scaling laws for thrust coefficients, power coefficients, and efficiencies were obtained for a rigid foil undergoing oscillatory heaving or pitching motions. For sinusoidal, continuous motions, water tunnel experiments on a nominally two-dimensional rigid foil confirmed the scaling laws, as the data showed excellent collapse. Viscous drag was also considered; it was seen to add a constant negative offset to the thrust coefficient, but it completely changed the behavior of the efficiency curves. Viscous drag causes the universally observed sharp decrease in efficiency for less intense motions, and our scaling laws capture this behavior.

The effects of waveform shape on propulsive performance were also studied. Although the waveform shape may significantly alter the propulsive performance, we found that, for the family of waveform shapes considered here, the thrust and power for different waveform shapes can be collapsed by a scaling based on the peak velocity of the trailing edge of the foil. Coupled with the scaling result for sinusoidal motions, this gives a scaling which can collapse propulsive performance for a wide range of motions.

The effects of waveform shape on propulsive performance were also studied. Although the waveform shape may significantly alter the propulsive performance, we found that, for the family of waveform shapes considered here, the thrust and power for different waveform shapes can be collapsed by a scaling based on the peak velocity of the trailing edge of the foil. Coupled with the scaling result for sinusoidal motions, this gives a scaling which can collapse propulsive performance for a wide range of motions.

In future work, we will consider the scaling of combined heave/pitch motions, the effects of aspect ratio, and the effects of flexibility.

This work was supported under ONR MURI grant N00014-14-1-0533 (Program Manager Robert Brizzolara).

REFERENCES

Barrett, D. S., Triantafyllou, M. S., Yue, D. K. P., Grosenbaugh, M. A. & Wolfgang, M. J. 1999 Drag reduction in fish-like locomotion. *Journal of Fluid Mechanics* **392**, 183–212.

Dewey, P. A., Boschitsch, B. M., Moored, K. W., Stone, H. A. & Smits, A. J. 2013 Scaling laws for the thrust production of flexible pitching panels. *Journal of Fluid Mechanics* **732**, 29–46.

Floryan, D., Van Buren, T., Rowley, C. W. & Smits, A. J. 2017*a* Scaling the propulsive performance of heaving and pitching foils. *Journal of Fluid Mechanics* p. under review.

Floryan, D., Van Buren, T. & Smits, A. J. 2017*b* Forces and energetics of intermittent swimming. *Acta Mechanica Sinica* p. under review.

Garrick, I. E. 1936 Propulsion of a flapping and oscillating airfoil. *Tech. Rep.* 567. NACA.

Lighthill, M. J. 1970 Aquatic animal propulsion of high hydromechanical efficiency. *Journal of Fluid Mechanics* **44** (02), 265–301.

Read, D. A., Hover, F. S. & Triantafyllou, M. S. 2003 Forces on oscillating foils for propulsion and maneuvering. *Journal of Fluids and Structures* **17** (1), 163–183.

Theodorsen, T. 1935 General theory of aerodynamic instability and the mechanism of flutter. *Tech. Rep.* 496; originally published as ARR-1935. NACA.

Triantafyllou, M. S., Hover, F. S., Techet, A. H. & Yue, D. K. 2005 Review of hydrodynamic scaling laws in aquatic locomotion and fishlike swimming. *Applied Mechanics Reviews* **58** (4), 226–237.

Van Buren, T., Floryan, D., Quinn, D. & Smits, A. J. 2017*a* Nonsinusoidal gaits for unsteady propulsion. *Physical Review Fluids* p. under review.

Van Buren, T., Wei, N., Floryan, D. & Smits, A. J. 2017*b* Swimming speed has little impact on fish-like swimming performance. *Journal of Fluid Mechanics* p. under review.

Weihs, D. 1974 Energetic advantages of burst swimming of fish. *Journal of Theoretical Biology* **48** (1), 215–229.